Transfer of angular spectrum and image formation in spontaneous parametric down-conversion

C. H. Monken,* P. H. Souto Ribeiro, and S. Pádua
Departamento de Física, Universidade Federal de Minas Gerais, Caixa Postal 702, Belo Horizonte, MG 30123-970, Brazil

(Received 30 October 1997)

We show that the two-photon state generated in the process of spontaneous parametric down-conversion in a thin crystal carries information about the angular spectrum of the pump beam. This information transfer allows one to control the transverse correlation properties of the down-converted fields by manipulating the pump field, with consequences for a broad class of experiments. The effect is demonstrated theoretically and experimentally, in connection with the formation of fourth-order images by the down-converted beams. [S1050-2947(98)03004-2]

PACS number(s): 42.50.Ar

Transverse properties of the fields generated by spontaneous parametric down-conversion have received attention from a number of groups, from both theoretical and experimental points of view [1–14]. Most of this interest is due to the rich variety of fourth-order interference effects shown by the entangled two-photon state generated by that system, some of them exhibiting nonlocal features [15].

Some effects related to the focusing of the pump beam were studied by Klyshko [1,2], and Pittman and co-workers [7,9]. A detailed account of the transverse correlation of the down-converted beams under the action of passive linear optical systems in their paths was recently given by Rubin [12].

In this work we present a treatment which links the transverse properties of the down-converted beams with those of the pump beam. We show that when the crystal is short enough in the pump beam propagation direction, the angular spectrum of the pump beam is transferred to the two-photon state generated by the down-conversion process. The angular spectrum transfer gives rise to a new effect, which we have demonstrated experimentally—the image transfer from the pump to the two-photon down-converted field. This effect offers the possibility of controlling the structure of the transverse profile of the coincidence detection without disturbing the intensity profile, and without any additional optics in the down-converted beams. As its potential applications, we can cite experimental tests of Einstein's local realism [16,17], quantum interferometry [18], and quantum cryptography [19], among others.

Let us consider the nonlinear crystal in the form of a box centered at the origin, with sides L_1, L_2, and L_3 parallel to the x, y, and z axes, respectively. The pumping is provided by a continuous monochromatic laser beam, whose cross section is entirely contained in the nonlinear medium, propagating along the positive-z axis. For simplicity, we will assume that the crystal is embedded in an index-matching passive medium, so that the wave vectors are nearly the same in both media. The nonlinearity and pump power will be considered weak enough to assure a first-order perturbative approach [20]. If the quantization volume is very large, one can write the following expression for the state generated by spontaneous parametric down-conversion, based on the treatment given in Ref. [20]:

$$|\psi\rangle = |\mathrm{vac}\rangle + \mathrm{const} \times \int d\mathbf{k}_s \int d\mathbf{k}_i \mathrm{sinc}\frac{1}{2}(\omega_s + \omega_i - \omega_p)t \times \Phi(\mathbf{k}_s, \mathbf{k}_i)|1;\mathbf{k}_s\rangle|1;\mathbf{k}_i\rangle, \tag{1}$$

where

$$\Phi(\mathbf{k}_s,\mathbf{k}_i) = \int d\mathbf{q}_p v(\mathbf{q}_p)\left[\frac{\omega_s\omega_i\omega_p}{n^2(\mathbf{k}_s)n^2(\mathbf{k}_i)n^2(\mathbf{k}_p)}\right]^{1/2} \times \prod_{j=1}^{3} \mathrm{sinc}\frac{1}{2}(\mathbf{k}_s+\mathbf{k}_i-\mathbf{k}_p)_j L_j . \tag{2}$$

$\mathbf{q}_p$ is the transverse (xy) component of the pump wave vector $\mathbf{k}_p$, $v(\mathbf{q}_p)$ is the angular spectrum of the pump beam, and $n(\mathbf{k}_j)$ are the refractive indices of the nonlinear medium for the modes s (signal), i (idler), and p (pump). It is known that the phase-matching conditions, expressed by the sinc functions in Eqs. (1) and (2) are satisfied in nonlinear crystals only for certain polarizations of the modes s, i, and p, characterizing two types of phase matching: type I ($o \rightarrow ee$) and type II ($o \rightarrow oe$ or $e \rightarrow oe$), where o (e) stands for ordinary (extraordinary) polarization, referring to the modes $p \rightarrow si$. The set of polarizations is implicit in Eqs. (1) and (2). We will consider only the monochromatic case, with $\omega_s + \omega_i = \omega_p$, so the time dependence of state (1) disappears. This approximation is justified by the fact that the only frequencies of interest are the ones defined by filters placed in front of the detectors, which can be very narrow interference filters. The following approximations will also be assumed. The pump beam has a narrow angular spectrum, and the down-converted modes are observed only in points close to the z axis (collinear phase matching), so that $|\mathbf{q}| \ll |\mathbf{k}|$ for the three modes involved. Under these approximations, the refractive indices $n(\mathbf{k}_p)$, $n(\mathbf{k}_s)$, and $n(\mathbf{k}_i)$ can be regarded as constants. Integral (2) then becomes

*Corresponding author. Electronic address: monken@fisica.ufmg.br

$$\Phi(\mathbf{k}_s,\mathbf{k}_i)=v(\mathbf{q}_s+\mathbf{q}_i)\operatorname{sinc}\frac{1}{2}\Big(\sqrt{k_s^2-q_s^2}+\sqrt{k_i^2-q_i^2}$$
$$-\sqrt{k_p^2-|\mathbf{q}_s+\mathbf{q}_i|^2}\Big)L_z. \tag{3}$$

If L_z is small compared to $|\mathbf{q}_s|^{-1}$ and $|\mathbf{q}_i|^{-1}$, $\Phi(\mathbf{k}_s,\mathbf{k}_i)$ can finally be written as

$$\Phi(\mathbf{k}_s,\mathbf{k}_i)\simeq v(\mathbf{q}_s+\mathbf{q}_i). \tag{4}$$

In this thin crystal approximation, only the transverse components of the momentum are conserved, and the angular spectrum of the pump beam is transferred to the two-photon state.

We now show that this transfer of the angular spectrum leads to the observation of images through the fourth-order correlation function of the down-converted fields. The photodetection coincidence rate $C(\mathbf{r}_s,\mathbf{r}_i)$ for very small detectors located at $\mathbf{r}_s$ and $\mathbf{r}_i$ is proportional to

$$\langle\psi|E^{(-)}(\mathbf{r}_s)E^{(-)}(\mathbf{r}_i)E^{(+)}(\mathbf{r}_i)E^{(+)}(\mathbf{r}_s)|\psi\rangle. \tag{5}$$

If we write the electric-field operator as

$$E^{(+)}(\mathbf{r})=\int d\mathbf{q}\; a(\mathbf{q})e^{i(\mathbf{q}\cdot\boldsymbol{\rho}+\sqrt{k^2-\rho^2}z)}, \tag{6}$$

where $\boldsymbol{\rho}$ is the transverse component of $\mathbf{r}$, $C(\mathbf{r}_s,\mathbf{r}_i)$ will be found to be

$$C(\mathbf{r}_s,\mathbf{r}_i)=\text{const}\times|g(\mathbf{r}_s,\mathbf{r}_i)|^2, \tag{7}$$

where

$$g(\mathbf{r}_s,\mathbf{r}_i)=\int d\mathbf{q}_s\int d\mathbf{q}_i v(\mathbf{q}_s+\mathbf{q}_i)$$
$$\times e^{i(\mathbf{q}_s\cdot\boldsymbol{\rho}_s+\mathbf{q}_i\cdot\boldsymbol{\rho}_i+\sqrt{k_s^2-q_s^2}z_s+\sqrt{k_i^2-q_i^2}z_i)}. \tag{8}$$

Restricting the observation region to the limit $|\boldsymbol{\rho}|\ll|\mathbf{r}|$, and working out expression (8), $g(\mathbf{r}_s,\mathbf{r}_i)$ can be put in the form

$$g(\mathbf{r}_s,\mathbf{r}_i)=\int d\boldsymbol{\rho}\;\mathcal{W}(\boldsymbol{\rho})e^{-i(|\mathbf{k}_p|/2Z_o)|\mathbf{R}-\boldsymbol{\rho}|^2}, \tag{9}$$

apart from an irrelevant phase factor, provided that Z_o and $\mathbf{R}$ are given by

$$\frac{1}{Z_o}=\frac{|\mathbf{k}_s|}{|\mathbf{k}_p|}\frac{1}{z_s}+\frac{|\mathbf{k}_i|}{|\mathbf{k}_p|}\frac{1}{z_i}, \tag{10}$$

$$\mathbf{R}=\frac{Z_o}{z_s}\frac{|\mathbf{k}_s|}{|\mathbf{k}_p|}\boldsymbol{\rho}_s+\frac{Z_o}{z_i}\frac{|\mathbf{k}_i|}{|\mathbf{k}_p|}\boldsymbol{\rho}_i=\frac{1}{\mu_s}\boldsymbol{\rho}_s+\frac{1}{\mu_i}\boldsymbol{\rho}_i. \tag{11}$$

$\mathcal{W}(\boldsymbol{\rho})$ is the Fourier transform of $v(\mathbf{q})$, that is, the amplitude profile of the pump beam at $z=0$. The integral in Eq. (9) describes the propagation of $\mathcal{W}(\boldsymbol{\rho})$ from $z=0$ to $z=Z_o$ in the paraxial approximation (which we have already assumed). Therefore, the coincidence rate profile will be

$$C(\mathbf{r}_s,\mathbf{r}_i)=\text{const}\times|\mathcal{W}(\mathbf{R};Z_o)|^2, \tag{12}$$

that is, the intensity profile of the pump beam at $z=Z_o$ is transferred to the coincidence rate profile, in terms of the coordinate $\mathbf{R}$ given by Eq. (11). $\mathbf{R}$ is a weighted mean of $\boldsymbol{\rho}_s$ and $\boldsymbol{\rho}_i$, and μ_s and μ_i in Eq. (11) are magnification factors. If an optical system (apertures and lenses) is inserted into the pump beam before it reaches the crystal, leading it to form an image of some obstacle or aperture on the plane $z=Z_o$, this image will also be transferred to the coincidence rate profile. The definition of Z_o given by Eq. (10) can be regarded as the focusing condition of this fourth-order image.

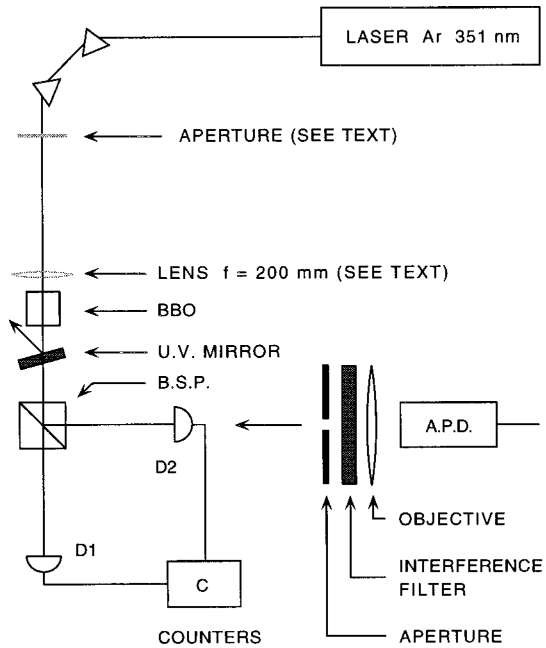

FIG. 1. Experimental setup.

It is interesting to note that the non-factorized dependence of $\mathcal{W}$ on $\boldsymbol{\rho}_s$ and $\boldsymbol{\rho}_i$ through $\mathbf{R}$ is a consequence of the entanglement between signal and idler. In the context of the above approximations, it is easy to show that the single-count rates in each detector are independent of $\boldsymbol{\rho}_s$ and $\boldsymbol{\rho}_i$, showing no second-order imaging.

Now let us suppose that one of the detectors (say the idler), instead of being punctual, has an active area defined by the aperture function $\mathcal{A}(\boldsymbol{\rho}_i)$. In this case, the coincidence rate (12) must be integrated over $\mathcal{A}$:

$$C(\mathbf{r}_s)=\text{const}\times\int d\boldsymbol{\rho}_i\mathcal{A}(\boldsymbol{\rho}_i)\left|\mathcal{W}\left(\frac{\boldsymbol{\rho}_s}{\mu_s}+\frac{\boldsymbol{\rho}_i}{\mu_i};Z_o\right)\right|^2. \tag{13}$$

This represents the convolution

$$C(\mathbf{r}_s)=\text{const}\times\mathcal{A}\left(\frac{\boldsymbol{\rho}_i}{\mu}\right)*\left|\mathcal{W}\left(\frac{\boldsymbol{\rho}_s}{\mu_s};Z_o\right)\right|^2, \tag{14}$$

where $\mu=-\mu_i/\mu_s$. An interesting particular case of Eq. (14) occurs when Z_o lies on the focus of a lens placed in the Gaussian pump beam. In this situation, $\mathcal{W}(\mathbf{R};Z_o)$ has a narrow Gaussian shape that can be approximated by $\delta(\mathbf{R})$, and the coincidence rate profile will reproduce the aperture function

$$C(\mathbf{r}_s)=\text{const}\times\mathcal{A}\left(-\frac{\boldsymbol{\rho}_s}{\mu_s}\right). \tag{15}$$

This kind of image was in fact observed by Pittman *et al.* [9].

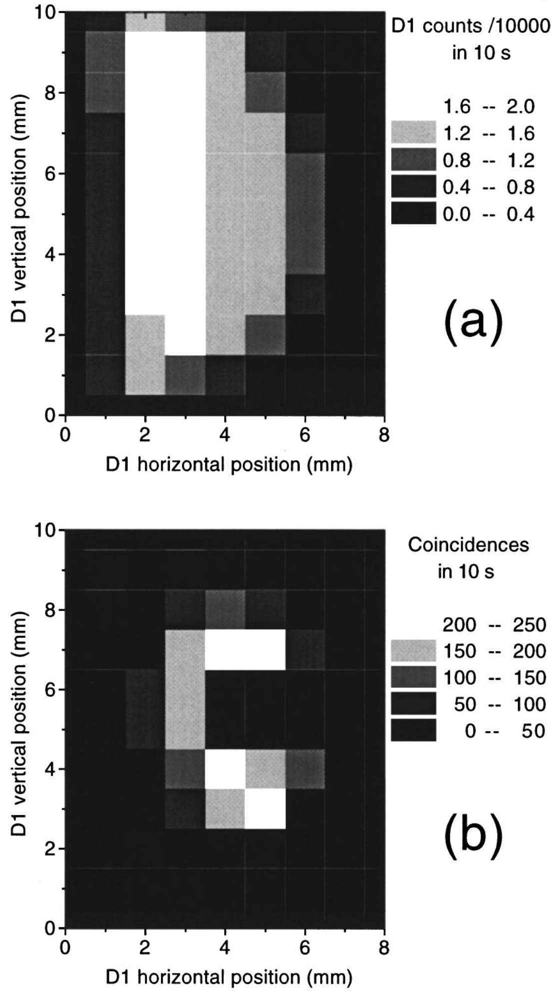

FIG. 2. Representation in density plots of the measured $D1$ single counts (a) and $D1$-$D2$ coincidence counts (b) in a matrix of 8×10 pixels, with sampling times of 10 s per pixel. The image of a C-shaped aperture formed by the pump beam in the plane of the detectors is transferred to the coincidence profile.

An experiment, whose setup is shown in Fig. 1, was performed to demonstrate the angular spectrum and image transfer effect just described. A 7-mm-long BBO nonlinear crystal is pumped by a 100-mW argon laser operating at $\lambda_p=351.1$ nm. The crystal, whose optical axis lies in a horizontal plane, is cut for collinear type-II phase matching, with $\lambda_s=\lambda_i=702.2$ nm. The down-converted beams emerge from the crystal with orthogonal linear polarizations, and are separated from the pump by a uv mirror, placed right at the crystal output. A beam-splitter polarizer directs signal (here identified with the extraordinary polarization) and idler (ordinary) beams onto detectors $D1$ and $D2$, respectively, both mounted on X-Y micrometric translation stages. In front of each detector there is an arrangement composed by a variable aperture, which can be a slit or a circular orifice, followed by an interference filter of 1-nm bandwidth, and a microscope objective focused on the detector's active area. The response of this detection system as a function of the wave-vector incidence angle was measured with the help of an attenuated laser beam, and was found to be flat over an interval of 1.0° centered at 0°. Detectors $D1$ and $D2$ are connected to single and coincidence counters, with a resolving time of 10 ns.

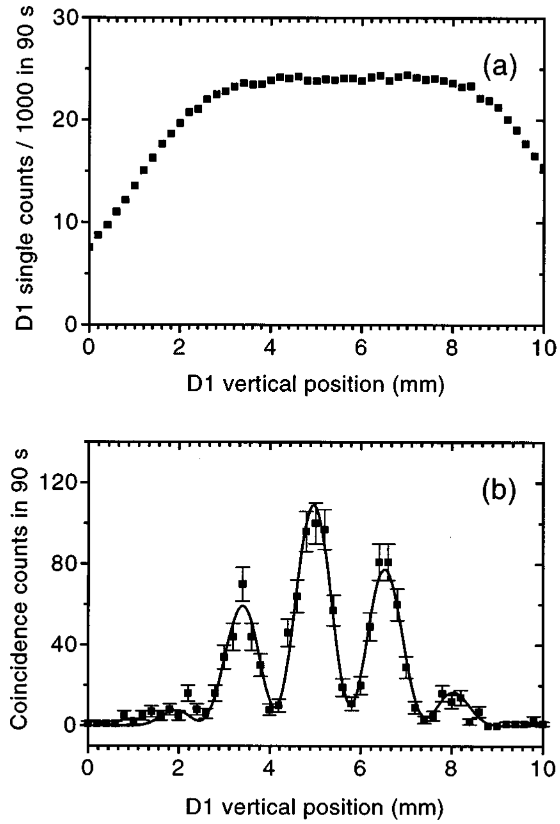

FIG. 3. Measured $D1$ single counts (a) and $D1$-$D2$ coincidence counts (b) when a double slit is placed in the pump beam before it reaches the crystal, producing a Young interference pattern in the plane of the detectors. Each point corresponds to a sampling time of 90 s. The solid line is a fit of the double-slit interference pattern with visibility of 82%.

In the first measurement, Z_o was chosen to be 450 mm, and $\mu_s=\mu_i=2$, that is, $z_s=z_i=Z_o$ as defined by expression (10). A lens of $f=200$ mm was placed in the pump beam at 50 mm from the crystal in order to form, on the plane of the detectors, the image of an aperture placed 330 mm from it. The aperture was chosen to have roughly the shape of the letter C, with a 2-mm height, producing an image of about 3 mm in the plane of the detectors. Detectors entrance apertures were set to be circular orifices of 1-mm diameter. Detector $D2$ was held fixed, whereas $D1$ scanned a matrix of 8 mm horizontal by 10 mm vertical, in steps of 1 mm. Figure 2 shows a representation in density plots of the measured $D1$ single counts (a) and $D1$-$D2$ coincidence counts (b) in a matrix of 8×10 pixels, with sampling times of 10 s per pixel. The fourth-order (coincidence) image of the aperture is clearly seen, with no second-order (single count) counterpart. The magnification factor of 2 is experimentally confirmed.

In a second experiment, the lens was removed, and two parallel slits 0.13 mm wide, separated by 0.33 mm, were placed in the pump beam, 310 mm from the crystal. This double slit produces Young interference fringes in the plane of the detectors. The entrance aperture of $D1$ and $D2$ were replaced by single slits 0.10 mm wide for $D1$ and 0.15 mm wide for $D2$, oriented parallel to the double slit (in the horizontal). $D2$ was held fixed as in the first experiment, while $D1$ was scanned vertically in steps of 0.2 mm. Figure 3 shows the results, with sampling times of 90 s per point.

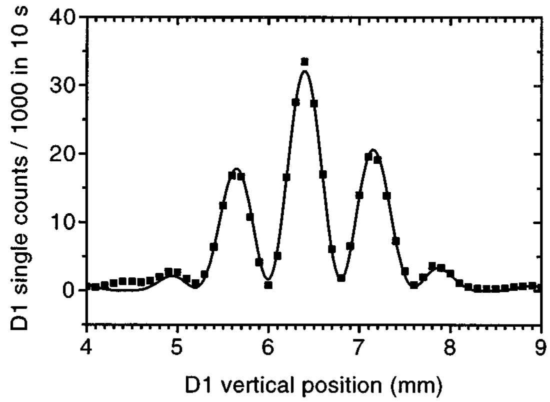

FIG. 4. The pump beam (uv) Young interference pattern measured by $D1$, with a fluorescent plastic behind its entrance slit. The solid line is a fit of the double-slit interference pattern, with a visibility of 89%.

Again, the fourth-order image shows up with no second-order counterpart. For comparison purposes, the pump beam interference pattern was registered by $D1$, and the results are shown in Fig. 4. For this measurement, the uv mirror was removed, the pump intensity reduced, and a thin transparent layer of fluorescent plastic was placed behind the $D1$ entrance slit. Comparing the interference pattern spatial periodicity in Fig. 3(b) with the one of Fig. 4, we find a magnification of 2, in agreement with the theory.

Let us analyze some consequences of the angular spectrum transfer. It provides a simple way to control the transverse spatial correlation between signal and idler photons, which can be of interest in practically all experiments with spontaneous parametric down-conversion. For example, in experiments to test the hypothesis of local realism employing pairs of photons, part of the so-called *detection loophole* is due to the insufficient transverse correlation between the photon pairs, as discussed by Santos [16]. Although this correlation has been taken for granted in parametric down-conversion, and little attention has been paid to it in the most recent experiments [21,22], the present work shows that it is strongly dependent on the pump beam. According to the theory developed here, the pump beam can be manipulated in order to maximize the transverse correlation and close this part of the loophole [23].

The image transfer process can also be of interest in the field of quantum cryptography. After a suitable modification of the downconversion source, it might be used to distribute a *key* for a hole image, instead of a bit stream, in the same lines described in Ref. [19].

The authors acknowledge financial support from the Brazilian agencies CNPq and FINEP.

[1] D. N. Klyshko, Zh. Eksp. Teor. Fiz. **83**, 1313 (1982) [Sov. Phys. JETP **56**, 753 (1982)].
[2] D. N. Klyshko, Zh. Eksp. Teor. Fiz. **94**, 82 (1988) [Sov. Phys. JETP **67**, 1131 (1988)].
[3] A. V. Belisnkiĭ and D. N. Klyshko, Pis'ma Zh. Eksp. Teor. Fiz. **105**, 487 (1998) [JETP **78**, 259 (1994)].
[4] T. P. Grayson and G. A. Barbosa, Phys. Rev. A **49**, 2948 (1994).
[5] P. H. S. Ribeiro, C. H. Monken, and G. A. Barbosa, Appl. Opt. **33**, 352 (1994).
[6] P. H. S. Ribeiro, S. Pádua, J. C. M. da Silva, and G. A. Barbosa, Phys. Rev. A **49**, 4176 (1994).
[7] T. B. Pittman, Y. H. Shih, D. V. Strekalov, and A. V. Sergienko, Phys. Rev. A **52**, R3429 (1995).
[8] D. V. Strekalov, A. V. Sergienko, D. N. Klyshko, and Y. H. Shih, Phys. Rev. Lett. **74**, 3600 (1995).
[9] T. B. Pittman *et al.*, Phys. Rev. A **53**, 2804 (1996).
[10] A. Joobeur, B. E. A. Saleh, T. S. Larchuk, and M. Teich, Phys. Rev. A **53**, 4360 (1996).
[11] P. H. S. Ribeiro and G. A. Barbosa, Phys. Rev. A **54**, 3499 (1996).
[12] M. Rubin, Phys. Rev. A **54**, 5349 (1996).
[13] J. Rehacek and J. Perina, Opt. Commun. **125**, 82 (1996).
[14] G. A. Barbosa, Phys. Rev. A **54**, 4473 (1996).
[15] For a review, see J. Perina, Z. Hradil, and B. Jurco, *Quantum Optics and Fundamentals of Physics* (Kluwer, Dordrecht, 1994).
[16] E. Santos, Phys. Rev. A **46**, 3646 (1992).
[17] P. G. Kwiat, P. H. Eberhard, A. M. Steinberg, and R. Y. Chiao, Phys. Rev. A **49**, 3209 (1994).
[18] *Quantum Interferometry*, edited by F. D. Martini, G. Denardo, and Y. Shih (VCH, Weinheim, 1996).
[19] A. K. Ekert, Phys. Rev. Lett. **67**, 661 (1991).
[20] C. K. Hong and L. Mandel, Phys. Rev. A **31**, 2409 (1985).
[21] J. R. Torgerson, D. Branning, C. H. Monken, and L. Mandel, Phys. Lett. A **204**, 323 (1995).
[22] P. G. Kwiat *et al.*, Phys. Rev. Lett. **75**, 4337 (1995).
[23] An experiment in this subject is currently in progress in our group.